Article

Homoleptic Cyclometalated Iridium Complexes with Highly Efficient Red Phosphorescence and Application to Organic Light-Emitting Diode

Akira Tsuboyama, Hironobu Iwawaki, Manabu Furugori, Taihei Mukaide, Jun Kamatani, Satoshi Igawa, Takashi Moriyama, Seishi Miura, Takao Takiguchi, Shinjiro Okada, Mikio Hoshino, and Kazunori Ueno

J. Am. Chem. Soc., **2003**, 125 (42), 12971-12979• DOI: 10.1021/ja034732d • Publication Date (Web): 27 September 2003

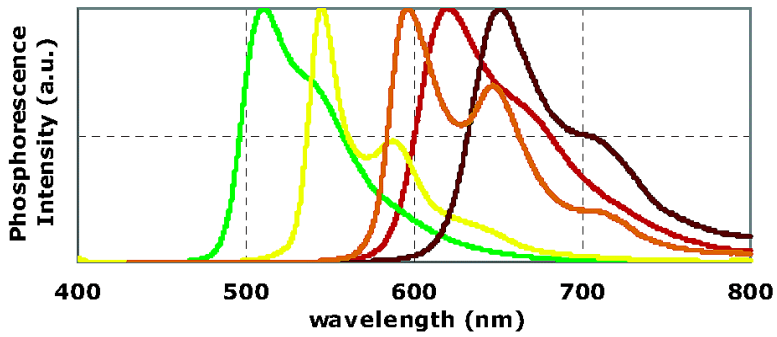

More About This Article

Additional resources and features associated with this article are available within the HTML version:

- Supporting Information
- Links to the 36 articles that cite this article, as of the time of this article download
- Access to high resolution figures
- Links to articles and content related to this article
- Copyright permission to reproduce figures and/or text from this article

View the Full Text HTML

J|A|C|S
ARTICLES
Published on Web 09/27/2003

Homoleptic Cyclometalated Iridium Complexes with Highly Efficient Red Phosphorescence and Application to Organic Light-Emitting Diode

Akira Tsuboyama,*,† Hironobu Iwawaki,† Manabu Furugori,† Taihei Mukaide,† Jun Kamatani,† Satoshi Igawa,† Takashi Moriyama,† Seishi Miura,† Takao Takiguchi,† Shinjiro Okada,† Mikio Hoshino,‡ and Kazunori Ueno†

Contribution from OL Project, Canon Inc., Atsugi, Kanagawa 243-0193, Japan, and The Institute of Physical and Chemical Research, Wako, Saitama 351-0198, Japan

Received February 18, 2003; E-mail: tsuboyama.akira@canon.co.jp

Abstract: Phosphorescence studies of a series of facial homoleptic cyclometalated iridium(III) complexes have been carried out. The complexes studied have the general structure Ir(III)(C−N)$_3$, where (C−N) is a monoanionic cyclometalating ligand: 2-(5-methylthiophen-2-yl)pyridinato, 2-(thiophen-2-yl)-5-trifluoromethylpyridinato, 2,5-di(thiophen-2-yl)pyridinato, 2,5-di(5-methylthiophen-2-yl)pyridinato, 2-(benzo[*b*]-thiophen-2-yl)pyridinato, 2-(9,9-dimethyl-9*H*-fluoren-2-yl)pyridinato, 1-phenylisoquinolinato, 1-(thiophen-2-yl)isoquinolinato, or 1-(9,9-dimethyl-9*H*-fluoren-2-yl)isoquinolinato. Luminescence properties of all the complexes at 298 K in toluene are as follows: quantum yields of phosphorescence $\Phi_p = 0.08-0.29$, emission peaks $\lambda_{max} = 558-652$ nm, and emission lifetimes $\tau = 0.74-4.7$ μs. Bathochromic shifts of the Ir(thpy)$_3$ family [the complexes with 2-(thiophen-2-yl)pyridine derivatives] are observed by introducing appropriate substituents, e.g., methyl, trifluoromethyl, or thiophen-2-yl. However, Φ_p of the red emissive complexes ($\lambda_{max} > 600$ nm) becomes small, caused by a significant decrease of the radiative rate constant, k_r. In contrast, the complexes with the 1-arylisoquinoline ligands are found to have marked red shifts of λ_{max} and very high Φ_p (0.19−0.26). These complexes are found to possess dominantly ^{3}MLCT (metal-to-ligand charge transfer) excited states and have k_r values approximately 1 order of magnitude larger than those of the Ir(thpy)$_3$ family. An organic light-emitting diode (OLED) device that uses Ir(1-phenylisoquinolinato)$_3$ as a phosphorescent dopant produces very high efficiency (external quantum efficiency $\eta_{ex} = 10.3\%$ and power efficiency 8.0 lm/W at 100 cd/m^2) and pure-red emission with 1931 CIE (Commission Internationale de L'Eclairage) chromaticity coordinates ($x = 0.68$, $y = 0.32$).

Introduction

In recent decades, the photophysics of cyclometalated metal complexes has been the subject of extensive studies. These complexes have attracted much attention because of their long-lived excited states and high luminescence quantum yields applicable to photoreductants,[1] oxygen sensors,[2] and emissive materials.[3,4] They include both square planar d^8 complexes of Pt(II),[3−8] Pd(II),[7,8] and Au(III)[9] and octahedral d^6 complexes of Ru(II),[10] Rh(III),[6,11,12] Re(I),[15] Ir(III),[1,2,11−14] and Pt(IV).[4,6,7] The strong spin−orbit coupling caused by heavy metal ions incorporated in the complexes results in efficient intersystem crossing from the singlet to the triplet excited state. In 1985, King et al.[1] first synthesized triply coordinated neutral *fac*-Ir-

† Canon Inc.
‡ The Institute of Physical and Chemical Research.

(1) King, K. A.; Spellane, P. J.; Watts, R. J. *J. Am. Chem. Soc.* **1985**, *107*, 1431−1432.
(2) Di Marco, G.; Lanza, M.; Mamo, A.; Stefio, I.; Di Pietro, C.; Romeo, G.; Campagna, S. *Anal. Chem.* **1998**, *70*, 5019−5023.
(3) (a) Maestri, M.; Sandrini, D.; Balzani, V.; Chassot, L.; Jolliet, P.; von Zelewsky, A. *Chem. Phys lett.* **1985**, *122* (4), 375−379. (b) Bär, L.; Gliemann, G.; Chassot, L.; von Zelewsky, A. *Chem. Phys. Lett*. **1986**, *123* (4), 264−267. (c) Sandrini, D.; Maestri, M.; Balzani, V.; Chassot, L.; von Zelewsky, A. *J. Am. Chem. Soc*. **1987**, *109*, 7720−7724. (d) Chassot, L.; von Zelewsky, A. *Inorg. Chem.* **1987**, *26*, 2814−2818. (e) Brooks, J.; Babayan, Y.; Lamansky, S.; Djurovich, P. I.; Tsyba, I.; Bau, R.; Thompson, M. E. *Inorg. Chem*. **2002**, *41* (12), 3055−3066.
(4) Chassot, L.; von Zelewsky, A.; Sandrini, D.; Maestri, M.; Balzani, V. *J. Am. Chem. Soc.* **1986**, *108*, 6084−6085.
(5) (a) Chassot, L.; Müller, E.; von Zelewsky, A. *Inorg. Chem.* **1984**, *23*, 4249−4253. (b) Maestri, M.; Sandrini, D.; Balzani, V.; von Zelewsky, A.; Deuschel-Cornioley, C.; Jolliet, P. *Helv. Chim. Acta* **1988**, *71*, 1053−1059.
(6) Barigelletti, F.; Sandrini, D.; Maestri, M.; Balzani, V.; von Zelewsky, A.; Chassot, L.; Jolliet, P.; Maeder, U. *Inorg. Chem.* **1988**, *27*, 3644−3647.
(7) Gianini, M.; Forster, A.; Haag, P.; von Zelewsky, A.; Stoeckli-Evans, H. *Inorg. Chem.* **1996**, *35*, 4889−4895.
(8) (a) Cronioley-Deuschel, C.; von Zelewsky, A. *Inorg. Chem*. **1987**, *26*, 3354−3358. (b) Jolliet, P.; Gianini, M.; von Zelewsky, A.; Bernardinelli, G.; Stoeckli-Evans, H. *Inorg. Chem*. **1996**, *35*, 4883−4888. (c) Gianini, M.; von Zelewsky, A.; Stoeckli-Evans, H. *Inorg. Chem.* **1997**, *36*, 6094−6098.
(9) (a) Cinellu, M. A.; Zucca, A.; Stoccoro, S.; Minghetti, G.; Manassero, M.; Sansoni, M. *J. Chem. Soc., Dalton Trans.* **1995**, 2865−2872. (b) Bonnardel, P. A.; Parish, R. V.; Pritchard, R. G. *J. Chem. Soc., Dalton Trans.* **1996**, 3185−3193. (c) Fuchita, Y.; Ieda, H.; Tsunemune, Y.; Kinoshita-Nagaoka, J.; Kawano, H. *J. Chem. Soc., Dalton Trans*. **1998**, 791−796. (d) Parish, R. V.; Wright, J. P.; Pritchard, R. G. *J. Organomet. Chem.* **2000**, *596*, 165−176.
(10) (a) Reveco, P.; Schmehl, R. H.; Cherry, W. R.; Fronczek, F. R.; Selbin, J. *Inorg. Chem.* **1985**, *24*, 4078−4082. (b) Reveco, P.; Medley, J. H.; Garber, A. R.; Bhacca, N. S.; Selbin, J. *Inorg. Chem.* **1985**, *24*, 1096−1099.
(11) (a) Sprouse, S.; King, K. A.; Spellane, P. J.; Watts, R. J. *J. Am. Chem. Soc.* **1984**, *106*, 6647−6653. (b) Ohsawa, Y.; Sprouse, S.; King, K. A.; DeArmond, M. K.; Hanck, K. W.; Watts, R. J. *J. Phys. Chem.* **1987**, *91*, 1047−1054.
(12) Colombo, M. G.; Brunold, T. C.; Riedener, T.; Güdel, H. U.; Förtsch, M.; Bürgi, H. *Inorg. Chem*. **1994**, *33*, 545−550.

$(ppy)_3$ (*fac*-tris[2-phenylpyridinato]Ir(III)) and investigated its photophysical and photochemical properties. $Ir(ppy)_3$ in degassed toluene shows very strong phosphorescence ($\lambda_{max} = 514$ nm, phosphorescence yield $\Phi_p = 0.4$) emitted from the predominantly ^{3}MLCT (metal-to-ligand charge transfer) excited state at room temperature. Afterward, Colombo et al.[12] reported that *fac*-$Ir(thpy)_3$ (*fac*-tris[2-(thiophen-2-yl)pyridinato]Ir(III)) exhibits strong phosphorescence from the predominantly $^3\pi-\pi^*$ excited state.

In 1999, Baldo et al.[16] made an organic light-emitting diode (OLED) with *fac*-$Ir(ppy)_3$ as a green phosphorescent dopant. The OLED device can utilize all of the electrogenerated singlet and triplet excitons, leading to ca. 100% internal quantum efficiency (η_{in}). More recently, a green device with η_{in} of nearly 100% has also been reported[17] with the use of a heteroleptic complex, $(ppy)_2$Ir(acac) (bis[2-phenylpyridinato]Ir(III)(acetylacetonate)), as a phosphorescent dopant. Interestingly, Adachi et al.[18] made a red-phosphorescent OLED with the use of $(btpy)_2$Ir(acac) (bis[2-(benzo[*b*]thiophen-2-yl)pyridinato]Ir(III)-(acetylacetonate)) as a dopant. The red OLED provided pure-red electroluminescence [CIE coordinates $(x, y) = (0.68, 0.32)$] with $\eta_{ex} = 7\%$.

To fabricate highly efficient red-emissive OLEDs, it is necessary to search for red-emissive metal complexes with large luminescence quantum yields. However, it is not easy to find such a red-emissive complex, since the luminescence quantum yields tend to decrease with an increase in the emission peak wavelength according to the energy gap law.[19]

The purpose of the present study is the molecular design of a highly efficient red-phosphorescent complex suitable for red OLED devices. In addition to high phosphorescence efficiency, the complex should possess high thermal stability for device fabrication and stable device performance. We particularly focused our attention on designing metal complexes that provide red emission from an MLCT excited state.

Experimental Section

^{1}H NMR spectra were recorded on a Bruker DPX-400 NMR spectrometer operating at 400 MHz. Elemental analysis was carried out with an elemental analyzer Vario EL CHNOS from Elementar Co.

Photoluminescence spectra were recorded on a Hitachi F4500 fluorescence spectrometer. Spectral data were corrected with the use of emission spectra of $Ir(ppy)_3$ and $Ir(piq)_3$ (tris[1-phenylisoquinolinato-C_2,N]iridium(III)) measured by a spectroradiometer SR1 from Topcon Ltd. Phosphorescence quantum yields were determined at room temperature with the use of an N_2-saturated toluene solution of 10^{-5} M *fac*-$Ir(ppy)_3$ as a reference. Phosphorescence spectra at 77 K were measured in a toluene−ethanol−methanol (5:4:1) mixed solvent.

Emission lifetimes were measured by a Hamamatsu Photonics C4334 streakscope with excitation light ($\lambda = 337.1$ nm) from an N_2 laser (LN120C from Laser Photonics). UV−visible spectra were recorded on a Shimadzu UV3100S spectrophotometer. Thermogravimetric and differential thermal analysis (TG/DTA) was performed by a TG-DTA 2000S thermal analyzer (MAC Science Co.) under N_2 stream with a scanning rate of 10 °C/min.

Crystals of $Ir(piq)_3$ suitable for X-ray analysis were obtained from chloroform solutions at room temperature. Diffraction data were collected at 93 K on a Rigaku RAXIS−RAPID imaging plate diffractometer equipped with graphite-monochromated Mo Kα radiation ($\lambda = 0.71069$ Å). The crystal structure of $Ir(piq)_3$ was solved by the direct method using SIR88. The crystal structure was refined by the full-matrix least-squares method on F^2. All non-hydrogen atoms were refined anisotropically, while hydrogen atoms were refined isotropically. All analyses were performed by the crystallographic software package CrystalStructure. A summary of the refinement details and the resulting agreement factor is given in the Supporting Information. The iridium center of $Ir(piq)_3$ is octahedrally coordinated by three bidentate ligands with a facial structure and a 3-fold rotational axis passing through the iridium atom.

OLED devices were fabricated by the conventional vacuum deposition method under pressures of less than 10^{-4} Pa. The devices were made on an indium−tin oxide (ITO) film (15 Ω/cm^2, thickness 120 nm, from Nippon Sheet Glass Co.) with a 3.14 mm^2 round-patterned area. Voltage−current properties of devices were measured on a handmade circuit with an operational amplifier and a load resistance, a computer-controlled arbitrary waveform generator Yokogawa AG1200, and a digital oscilloscope Tektronix TDS420. Luminance of the OLEDs was measured with a luminance colorimeter BM-7 from Topcon Ltd.

Material Preparations

Ligand Synthesis. Reagent-grade 5-methylthiophene-2-boronic acid, thiophene-2-boronic acid, benzo[*b*]thiophene-2-boronic acid, phenylboronic acid, 2,5-dibromopyridine, 2-chloro-5-trifluoromethylpyridine, 2-bromopyridine, and isoquinoline-*N*-oxide were purchased from Aldrich Chemical Co. or Tokyo Kasei Kogyo Co. 1-Chloroisoquinoline and 2-iodo-9,9-dimethylfluorene were prepared according to previous papers.[20,21]

All the ligands studied here were prepared by the modified Suzuki coupling reactions.[22,23] Tetrakis(triphenylphosphine)palladium and aqueous sodium carbonate were used as a catalyst and a base, respectively, in all the coupling reaction. Scheme 1 outlines some examples of the synthetic processes of the ligands. Detailed procedures of the preparation, the ^{1}H NMR spectra, and chemical analysis data of the ligands are given in the Supporting Information.

Synthesis of Complexes. General Procedure. Complexes were synthesized according to a previous paper.[14] Tris(acetylacetonato)-iridium(III), $Ir(acac)_3$ (0.5 g, 1.0 mmol), and cyclometalating ligand (ca. 5 mmol) were dissolved in 50 mL of glycerol. The solution was refluxed under nitrogen stream for 6 h. After completion of the reaction, 1 M aqueous hydrochloric acid was added to the solution, resulting in precipitation of the product. Then the poduct was filtered, washed with water, and dried at 100 °C in vacuo. The purification of the product was made by silica gel column chromatography with $CHCl_3$ as an

(13) (a) Nord, G.; Hazell, A. C.; Harzell, R. G.; Farver, O. *Inorg. Chem.* **1983**, *22*, 3429−3434. (b) Garces, F. O.; King, K. A.; Watts, R. J. *Inorg. Chem.* **1988**, *27*, 3464−3471. (c) Wilde, A. P.; Watts, R. J. *J. Phys. Chem.* **1991**, *95*, 622−629. (d) Wilde, A. P.; King, K. A.; Watts, R. J. *J. Phys. Chem.* **1991**, *95*, 629−634. (e) Urban, R.; Krämer, R.; Mihan, S.; Polborn, K.; Wagner, B.; Beck, W. *J. Organomet. Chem.* **1996**, *517*, 191−200. (f) Colombo, M. G.; Güdel, H. U. *Inorg. Chem.* **1993**, *32*, 3081−3087. (g) Colombo, M. G.; Hauser, A.; Güdel, H. U. *Inorg. Chem.* **1993**, *32*, 3088−3092. (h) Neve, F.; Crispini, A.; Campagna, S.; Serroni, S. *Inorg. Chem.* **1999**, *38*, 2250−2258. (i) Neve, F.; Crispini, A.; Loiseau, F.; Campagna, S. *J. Chem. Soc., Dalton Trans.* **2000**, 1399−1401. (j) Neve, F.; Crispini, A.; Serroni, S.; Loiseau, F.; Campagna, S. *Inorg. Chem.* **2001**, *40*, 1093−1101.
(14) Dedeian, K.; Djurovich, P. I.; Garces, F. O.; Carlson, G.; Watts, R. J. *Inorg. Chem.* **1991**, *30*, 1685−1687.
(15) Spellane, P.; Watts, R. J.; Vogler, A. *Inorg. Chem.* **1993**, *32*, 5633−5636
(16) Baldo, M. A.; Lamansky, S.; Burrows, P. E.; Thompson, M. E.; Forrest, S. R. *Appl. Phys. Lett.* **1999**, *75* (1), 4−6.
(17) Adachi, C.; Baldo, M. A.; Thompson, M. E.; Forrest, S. R. *J. Appl. Phys.* **2001**, *90* (10), 5048−5051.
(18) Adachi, C.; Baldo, M. A.; Forrest, S. R.; Lamansky, S.; Thompson, M. E.; Kwong, R. C. *Appl. Phys. Lett.* **2001**, *78* (11), 1622−1624.
(19) (a) Meyer, T. J. *Pure Appl. Chem.* **1986**, *58* (9), 1193−1206. (b) Cummings, S. D.; Eisenberg, R. *J. Am. Chem. Soc.* **1996**, *118*, 1949−1960. (c) Casper, J. V.; Meyer, T. J. *J. Phys. Chem.* **1983**, *87*, 952−957.
(20) Shirota, Y.; Kinoshita, M.; Noda, T.; Okumoto, K.; Ohara, T. *J. Am. Chem. Soc.* **2000**, *122*, 11021−11022.
(21) Zhang, H.; Kwong, F. Y.; Tian, Y.; Chan, K. S. *J. Org. Chem.* **1998**, *63*, 6886−6890.
(22) Miyaura, N.; Suzuki, A. *Chem. Rev.* **1995**, *95*, 2457−2483.
(23) Lohse, O.; Thevenin, P.; Waldvogel, E. *Synlett* **1999**, *1*, 45−48.

Scheme 1. Synthesis of the Ligands

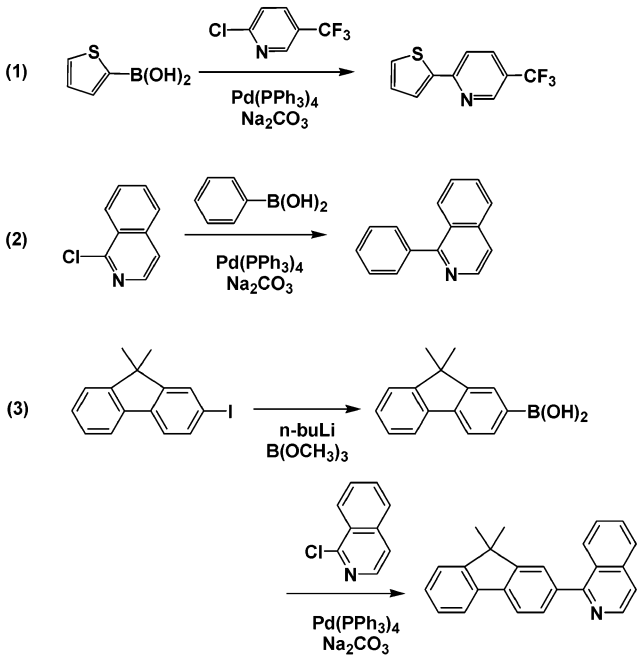

eluent. The yield of the product ranges from 11% to 45% based on $Ir(acac)_3$. The complexes used in this study are illustrated in Figure 1.

The ^1H NMR spectra and chemical analysis data of the complexes are as follows.

Ir(5m-thpy)$_3$ (1). Tris[2-(5-methylthiophen-2-yl)pyridinato-C^3,N]-iridium(III) [yield 21% with respect to $Ir(acac)_3$]: ^1H NMR ($CDCl_3$, 400 MHz) δ (ppm) 7.47−7.48 (m, 3H), 7.42(td, 3H, J = 8.0, 1.6 Hz), 7.30 (d, 3H, J = 8.0 Hz), 6.65 (m, 3H), 6.15 (s, 3H), 2.46 (s, 9H). Anal. Calcd for $C_{30}H_{24}IrN_3S_3$: C, 50.40; H, 3.38; N, 5.88. Found: C, 50.52; H, 3.65; N, 5.40.

Ir(t-5CF$_3$-py)$_3$ (2). Tris[2-(thiophen-2-yl)-5-trifluoromethylpyridinato-C^3,N]iridium(III) (yield 20%): ^1H NMR ($CDCl_3$, 400 MHz) δ (ppm) 7.69−7.75 (m, 6H), 7.57 (d, 3H, J = 8.5 Hz), 7.36 (d, 3H, J = 4.7 Hz), 6.40 (d, 3H, J = 4.7 Hz). Anal. Calcd for $C_{30}H_{15}F_9IrN_3S_3$: C, 41.09; H, 1.72; N, 4.79. Found: C, 41.40; H, 1.96; N, 4.69.

Ir(t-5t-py)$_3$ (3). Tris[2,5-di(thiophen-2-yl)pyridinato-C^3,N]iridium-(III) (yield 31%): ^1H NMR [$(CD_3)_2CO$, 400 MHz] δ (ppm) 8.02−8.05 (m, 6H), 7.66 (d, 3H, J = 8.5 Hz), 7.35−7.40 (m, 6H), 7.25 (m, 3H), 7.04 (m, 3H), 6.45 (d, 3H, J = 4.5 Hz). Anal. Calcd for $C_{39}H_{24}IrN_3S_6$: C, 50.96; H, 2.63; N, 4.57. Found: C, 51.47; H, 2.96; N, 4.25.

Ir(mt-5mt-py)$_3$ (4). Tris[2,5-di(5-methylthiophen-2-yl)pyridinato-C^3,N]iridium(III) (yield 38%): ^1H NMR ($CDCl_3$, 400 MHz) δ (ppm) 7.74 (s, 3H), 7.59 (dd, 3H, J = 8.5, 2.2 Hz), 7.31 (d, 3H, J = 8.5 Hz), 6.74 (d, 3H, J = 3.5 Hz), 6.59 (m, 3H), 6.21 (s, 3H), 2.48 (s, 9H), 2.40 (s, 9H). Anal. Calcd. for $C_{45}H_{36}IrN_3S_6$: C, 53.87; H, 3.62; N, 4.19. Found: C, 53.80; H, 3.72; N, 3.97.

Ir(btpy)$_3$ (5). Tris[2-(benzo[*b*]thiophen-2-yl)pyridinato-C^3,N]iridium-(III) (yield 23%): ^1H NMR ($CDCl_3$, 400 MHz) δ (ppm) 7.74 (d, 3H, J = 8.0 Hz), 7.49−7.55 (m, 6H), 7.32 (d, 3H, J = 6.6 Hz), 7.08 (td, 3H, J = 8.0, 1.4 Hz), 6.64−6.74 (m, 9H). Anal. Calcd. for $C_{39}H_{24}IrN_3S_3$: C, 56.91; H, 2.94; N, 5.11. Found: C, 56.99; H, 3.03; N, 4.77.

Ir(flpy)$_3$ (6). Tris[2-(9,9-dimethyl-9*H*-fluoren-2-yl)pyridinato-C^3,N]-iridium(III) (yield 21%): ^1H NMR ($CDCl_3$, 400 MHz) δ (ppm) 7.97 (d, 3H, J = 8.1 Hz), 7.73 (s, 3H), 7.56−7.60 (m, 6H), 7.34 (3H, d, J = 7.4 Hz), 7.21 (6H, m), 7.15 (3H, t, J = 7.2 Hz), 7.06 (3H, t, J = 7.4 Hz), 6.83 (3H, t, J = 6.2 Hz), 1.54 (9H, s), 1.47 (9H, s). Anal. Calcd for $C_{60}H_{48}IrN_3$: C, 71.83; H, 4.82; N, 4.19. Found: C, 71.50; H, 4.88; N, 4.04.

Ir(piq)$_3$ (7). Tris[1-phenylisoquinolinato-C^2,N]iridium(III) (yield 27%): ^1H NMR ($CDCl_3$, 400 MHz) δ (ppm) 8.96 (m, 3H), 8.18 (d, 3H, J = 7.9 Hz), 7.71 (m, 3H), 7.62 (m, 6H), 7.33 (d, 3H, J = 6.1 Hz), 7.09 (d, 3H, J = 6.1 Hz), 6.94−6.99 (m, 6H), 6.84 (t, 3H, J = 7.4 Hz). Anal. Calcd for $C_{45}H_{30}IrN_3$: C, 67.14; H, 3.76; N, 5.22. Found: C, 67.05; H, 3.80; N, 5.25.

Ir(tiq)$_3$ (8). Tris[1-thiophen-2-ylisoquinolinato-C^3,N]iridium(III) (yield 45%): ^1H NMR ($CDCl_3$, 400 MHz) δ (ppm) 8.94 (d, 3H, J = 8.2 Hz), 7.71 (m, 3H), 7.60−7.70 (m, 6H), 7.49 (d, 3H, J = 6.2 Hz), 7.38 (d, 3H, J = 4.7 Hz), 7.06 (d, 3H, J = 6.2 Hz), 6.55 (d, 3H, J = 4.7 Hz). Anal. Calcd for $C_{39}H_{24}IrN_3S_3$: C, 56.91; H, 2.94; N, 5.11. Found: C, 56.60; H, 2.99; N, 4.92.

Ir(fliq)$_3$ (9). Tris[1-(9,9-dimethyl-9*H*-fluoren-2-yl)isoquinolinato-C^3,N]iridium(III) (yield 32%): ^1H NMR ($CDCl_3$, 400 MHz) δ (ppm) 8.98 (d, 3H, J = 7.8 Hz), 8.25 (s, 3H), 7.73 (d, 3H, J = 6.9 Hz), 7.63−7.66 (m, 6H), 7.31−7.37 (m, 9H), 7.13−7.21 (m, 6H), 7.05−

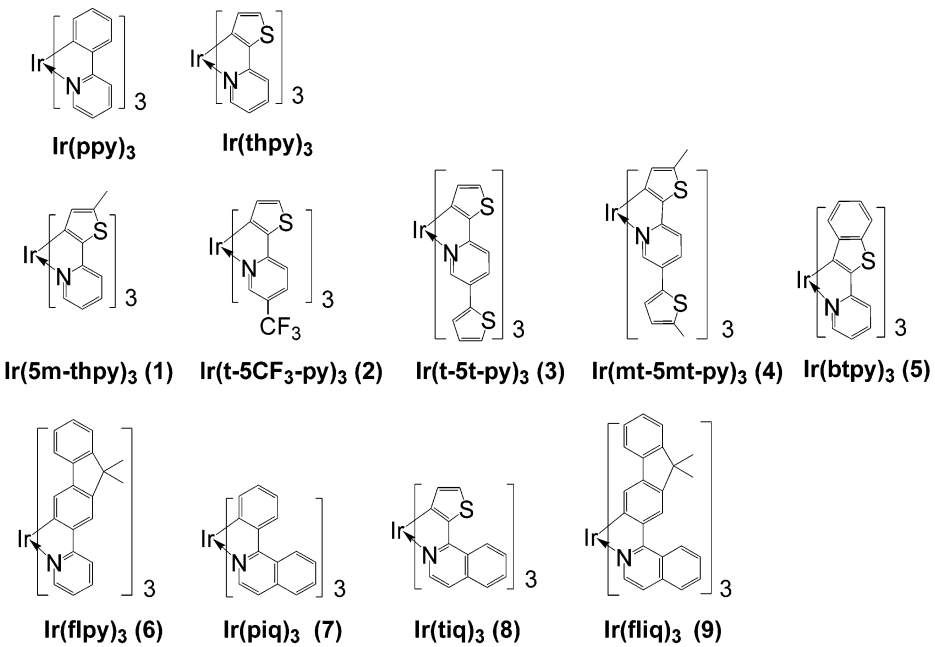

Figure 1. Ir complexes and their abbreviations used in the present study.

7.13 (m, 6H), 1.62 (s, 9H), 1.54 (s, 9H). Anal. Calcd for $C_{72}H_{54}IrN_3$: C, 74.97; H, 4.72; N, 3.64. Found: C, 74.48; H, 4.66; N, 3.44.

Results and Discussion

1. Thermal Stability. A vacuum deposition method is very convenient for making OLED devices. In this fabrication process, compounds used for the OLED devices are exposed to high temperatures (300−400 °C) when sublimed under vacuum. Thus, OLED materials should be stable even at high temperatures. When materials decompose in the deposition process, decomposition products may contaminate the OLED and cause poor device performance. Therefore, we have to carefully choose a thermally stable complex as a phosphorescent dopant.

Recently, Lamansky et al.[24,25] reported that a series of biscyclometalated Ir complexes with β-diketonato ancillary ligands such as $(ppy)_2Ir(acac)$ gave a wide range of emission colors with high phosphorescence yields comparable to those of triply cyclometalated homoleptic Ir complexes. We measured the decomposition temperatures of these complexes and triply cyclometalated homoleptic Ir complexes in order to examine whether these complexes are suitable for making OLED devices by vacuum deposition methods.

The decomposition temperature was determined from the TG/DTA curves measured under nitrogen stream. From the DTA curves of the complexes, we concluded that the weight reduction observed in the TG curves is caused by exothermic reactions of these complexes. Since thermal decomposition and sublimation are exothermic and endothermic, respectively, the weight reduction observed here is ascribed to the thermal decomposition. The 5% weight reduction temperatures ($\Delta T_{5\%}$) of these complexes are significantly different: 413 °C for $Ir(ppy)_3$, 341 °C for $(ppy)_2Ir(acac)$, and only 243 °C for $Ir(acac)_3$. These results indicate that the complexes with the acetylacetonato ligand tend to thermally decompose at relatively low temperatures. It is likely that the cyclometalated homoleptic iridium complexes are thermally more stable than the acetylacetonate complexes.

The homoleptic complexes $Ir(ppy)_3$ and $Ir(thpy)_3$ are known to afford strong green and yellow phosphorescence, respectively.[12] In the present study we designed new ligands in order to obtain highly efficient red-phosphorescent homoleptic iridium complexes.

2. Characterization of the Complexes. The ^1H NMR spectra of all complexes obtained here are consistent with a facial structure, which indicates that the number of coupled spins is equal to that of protons on one ligand because the three ligands are magnetically equivalent due to 3-fold symmetry.[12] The facial arrangement of the three ligands in $Ir(piq)_3$ **(7)** was confirmed by X-ray crystallography. Selected parameters of the molecular structure are listed in Table 1.

Figure 2 shows the ORTEP diagram of $Ir(piq)_3$ **(7)** given by X-ray analysis. It should be noted that the sterically crowded ligand results in large deformation with regard to the isoquinoline and phenyl rings in the complex. The deformation is caused by steric hindrance originating from the repulsion between two hydrogen atoms bound to the carbon atoms 7 and 11 (atom numbering is shown in Figure 2). The X-ray data show not only a large dihedral angle [C(8)−C(9)−C(10)−C(11) = 23°] between the two rings but also a strongly deformed isoquinoline ring out of the plane with a dihedral angle [C(7)−C(8)−C(9)−N(1)] of approximately 161°.

Table 1. Selected Structural Parameters for $Ir(piq)_3$ (**7**)

Bond Lengths (Å)	
Ir(1)−N(1)	2.135(5)
Ir(1)−C(15)	2.009(6)
N(1)−C(1)	1.374(8)
N(1)−C(9)	1.339(8)
Bond Angles (deg)	
N(1)−Ir(1)−C(15)	78.5(2)
Ir(1)−N(1)−C(1)	124.8(4)
Ir(1)−N(1)−C(9)	115.1(4)
Ir(1)−C(15)−C(10)	116.3(4)
C(1)−N(1)−C(9)	119.7(5)
Torsion Angles (deg)	
C(15)−Ir(1)−N(1)−C(9)	10.8(1)
N(1)−Ir(1)−C(15)−C(14)	173.2(1)
Ir(1)−N(1)−C(9)−C(8)	160.7(6)
C(3)−C(8)−C(9)−C(10)	−169.8(9)
C(8)−C(9)−C(10)−C(11)	22.9(2)
C(7)−C(8)−C(9)−N(1)	−161.2(9)

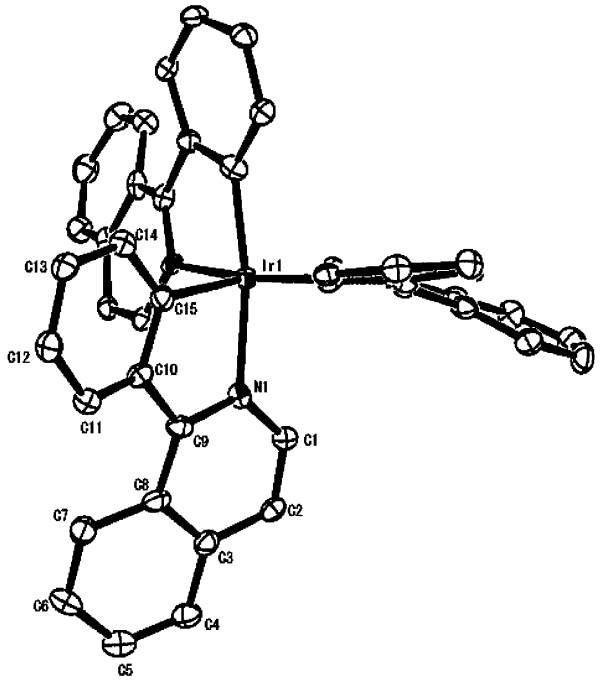

Figure 2. ORTEP diagram of $Ir(piq)_3$ (**7**) with the thermal ellipsoids representing a 50% probability level. Hydrogen atoms are omitted for clarity.

3. Photophysical Properties: 3.1. Absorption Spectra of Ir Complexes. Figure 3 shows the absorption spectra of $Ir(ppy)_3$, $Ir(mt\text{-}5mt\text{-}py)_3$ **(4)**, $Ir(piq)_3$ **(7)**, and $Ir(fliq)_3$ **(9)**. The absorption band of $Ir(piq)_3$ **(7)** located at ca. 420 nm is very similar in shape to that of $Ir(ppy)_3$ at ca. 380 nm. In comparison with the absorption band of $Ir(ppy)_3$, a marked bathochromic shift is observed for $Ir(piq)_3$ **(7)**, presumably owing to a large π conjugation system of the ligand piq.

$Ir(piq)_3$ **(7)** shows weak and broad absorption bands with molar absorption coefficients less than 3000 M^{-1} cm^{-1} in the wavelength region longer than 520 nm. According to the previous papers,[12,24] these weak bands located at long wave-

(24) Lamansky, S.; Djurovich, P.; Murphy, D.; Abdel-Razzaq, F.; Lee, H.; Adachi, C.; Burrows, P. E.; Forrest, S. R.; Thompson M. E. *J. Am. Chem. Soc.* **2001**, *123*, 4304−4312.
(25) Lamansky, S.; Djurovich, P.; Murphy, D.; Abdel-Razzaq; Kwong, R.; Tsyba, I.; Bortz, M.; Mui, B.; Bau, R.; Thompson, M. E. *Inorg. Chem.* **2001**, *40*, 1704−1711.

Table 2. Photophysical Properties of the Ir Complexes[a]

	absorption wavelengths, nm (logarithmic absorption coefficients, log [ϵ])	298 K					77 K	
		λ_{max}, nm	Φ_p	τ, μs	k_r, 10^5 s^{-1}	k_{nr}, 10^5 s^{-1}	λ_{peak}, nm	t, μs
Ir(ppy)$_3$		514	0.40	2.0	2.0	3.0	498, 534	6.5
Ir(thpy)$_3$		550	0.17	2.4	0.7	3.5	545, 566, 590, 614	8.2
Ir(5m-thpy)$_3$ (**1**)	309(4.9), 350(4.6), 404s(4.4), 460s(4.0), 511s(2.9)	558	0.08	0.99	0.8	9.3	553, 574, 599, 623	10.2
Ir(t-5CF$_3$-py)$_3$ (**2**)	313(4.8), 360(4.4), 403s(4.4), 472s(4.0), 526s(3.0)	563	0.19	1.1	1.7	7.2	557, 580, 604, 631	6.5
Ir(t-5t-py)$_3$ (**3**)	320s(4.8), 370s(4.4), 423(4.4), 472s(4.1)	613	0.12	4.6	0.3	1.9	605, 633, 662, 695	19.2
Ir(mt-5mt-py)$_3$ (**4**)	334(4.7), 390(4.4), 430s(4.3), 482s(4.1)	627	0.08	4.7	0.2	2.0	620, 649, 679, 715	10.8
Ir(btpy)$_3$ (**5**)	324s(4.6), 411(4.3), 472s(3.9)	596	0.12	4.0	0.3	2.2	586, 624, 640, 700	11.2
Ir(flpy)$_3$ (**6**)	327(4.3), 348(4.3), 413s(3.6)	545	0.29	1.2	2.5	6.0	537, 560, 584, 645	4.0
Ir(piq)$_3$ (**7**)	333s(4.2), 354s(4.1), 430(3.9), 483s(3.8), 550s(3.3), 600s(2.8)	620	0.26	0.74	3.6	9.9	603, 656	2.1
Ir(tiq)$_3$ (**8**)	333(4.5), 355(4.4), 437(4.3), 520s(3.8), 580s(2.9), 630s(2.8)	644	0.17	0.74	2.3	11.2	638, 663, 697	3.5
Ir(fliq)$_3$ (**9**)	360(4.9), 376(4.8), 450(4.4), 500s(4.1), 570s(3.8), 620s(3.0)	652	0.19	0.74	2.6	10.9	635, 693	2.1

[a] Absorption spectra were measured in aerated toluene solutions at 298 K. Luminescence lifetimes (τ) and quantum yields (Φ_p) in N_2-saturated toluene solutions were measured at 298 K. Wavelengths of excitation light are in the range of 400−450 nm. The k_r and k_{nr} values are calculated by eqs 2 and 3 on the assumption that Φ_{ISC} is 1.0. Phosphorescence lifetimes and spectra at 77 K were measured with the use of toluene/ethanol/methanol (5:4:1) solutions.

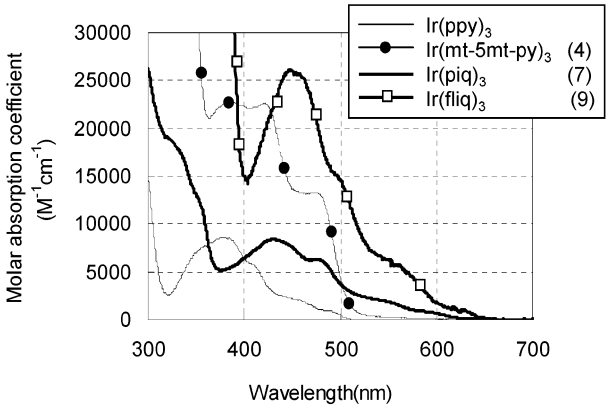

Figure 3. Absorption spectra of toluene solutions of Ir(ppy)$_3$, Ir(mt-5mt-py)$_3$ **(4)**, Ir(piq)$_3$ **(7)**, and Ir(fliq)$_3$ **(9)**.

lengths have been assigned to the ^{1}MLCT ← S_0 and ^{3}MLCT ← S_0 transitions of iridium complexes. Thus, the broad absorption shoulders at ca. 550 and 600 nm observed for Ir(piq)$_3$ **(7)** are likely to be ascribed to the ^{1}MLCT ← S_0 and the ^{3}MLCT ← S_0 transitions, respectively. The intensity of the ^{3}MLCT ← S_0 transition is close to that of ^{1}MLCT ← S_0, suggesting that the ^{3}MLCT ← S_0 transition is strongly allowed by S−T mixing due to spin−orbit coupling.[24] In analogy, the weak absorption shoulders of Ir(fiq)$_3$ **(9)** at 570 and 620 nm are, respectively, assumed to be attributed to the ^{1}MLCT ← S_0 and the ^{3}MLCT ← S_0 transitions. In the absorption spectrum of Ir(tiq)$_3$ **(8)**, the 630 nm band appears to be the ^{3}MLCT transition band. From these considerations, the lowest excited states of the complexes **7**−**9** are presumed to be the triplet MLCT excited states.

On the other hand, Ir(mt-5mt-py)$_3$ **(4)** does not exhibit distinct MLCT ← S_0 absorption bands in the wavelength region longer than 520 nm. Complexes **3** and **5**, which have large π conjugation systems of thiophen derivatives, exhibit absorption spectra similar to that of **4**. As in the case of Ir(thpy)$_3$ mentioned in the previous paper,[12] the intense absorption bands (log $\epsilon \sim$ 4.7) at ca. 320−340 nm observed for **3**−**5** are attributed to the $^1\pi-\pi^*$ ← S_0 transition and the broad and relatively weak absorption band in the range of 380−480 nm is attributed to the ^{1}MLCT ← S_0 transition.

Absorption peak wavelengths and the molar absorption coefficients of all complexes used in the present study are listed in Table 2. As expected from the molecular structures, the absorption spectra of **1** and **2** are very similar to that of Ir(thpy)$_3$. This fact suggests that the electronic nature of the lowest excited state is very similar among **1**, **2**, and Ir(thpy)$_3$. The lowest excited state of Ir(thpy)$_3$ has already been assigned to the dominantly $^3\pi-\pi^*$ excited state, and therefore the complexes **1** and **2** are likely to have the dominantly $^3\pi-\pi^*$ lowest excited state. On the basis of these considerations mentioned above, we suppose that the lowest excited states of complexes **1**−**5** with the thiophene derivative ligands can be assigned to the ligand-centered $^3\pi-\pi^*$ excited states.

3.2. Phosphorescence Spectra. Phosphorescence of mononuclear metal complexes originates from the ligand-centered excited state, metal-centered excited state, and MLCT excited state. For the cyclometalated Ir complexes, the wave function of the excited triplet state, Φ_T, responsible for phosphorescence is principally expressed as

$$\Phi_T = a\Phi(\mathrm{LC})_T + b\Phi(\mathrm{MLCT})_T \qquad (1)$$

where a and b are the normalized coefficients and $\Phi(\mathrm{LC})_T$ and $\Phi(\mathrm{MLCT})_T$ are the wave functions of the ligand-centered ($^3\pi-\pi^*$) and the MLCT excited triplet state, respectively. Equation 1 implies that the excited triplet states of the iridium complexes are a mixture of $\Phi(\mathrm{LC})_T$ and $\Phi(\mathrm{MLCT})_T$. The triplet excited state is attributed to the dominantly $^3\pi-\pi^*$ excited state when $a > b$ and the dominantly ^{3}MLCT excited state when $b > a$.

According to the previous works,[15,24] phosphorescence spectra from the ligand-centered $^3\pi-\pi^*$ state display vibronic progressions, while those from the ^{3}MLCT state are broad and featureless. Figure 4 shows the phosphorescence spectra of the Ir complexes observed at 298 and 77 K. The spectra measured at 298 K have two major phosphorescence peaks. At 77 K, the complexes **1**−**6** and Ir(thpy)$_3$ show phosphorescence spectra with well-resolved vibronic progressions between two major peaks. It seems that these complexes give phosphorescence from the dominantly ligand-centered $^3\pi-\pi^*$ excited state.

In comparison with the complexes **1**−**6** and Ir(thpy)$_3$, the phosphorescence spectra of the Ir complexes **7**−**9** and Ir(ppy)$_3$ measured at 298 K are broad and those measured at 77 K tend to lose fine vibronic progressions. This result indicates that the lowest excited triplet states of the complexes, Ir(ppy)$_3$ and **7**−**9**, gain larger contributions from the MLCT state than the complexes **1**−**6** and Ir(thpy)$_3$. Thus, as described previously, the lowest excited states of these complexes are likely to be dominantly the ^{3}MLCT excited state.

For ease of discussion, we divided the complexes studied here into two groups: the Ir thiophene/fluorene family, **1**−**6**, and

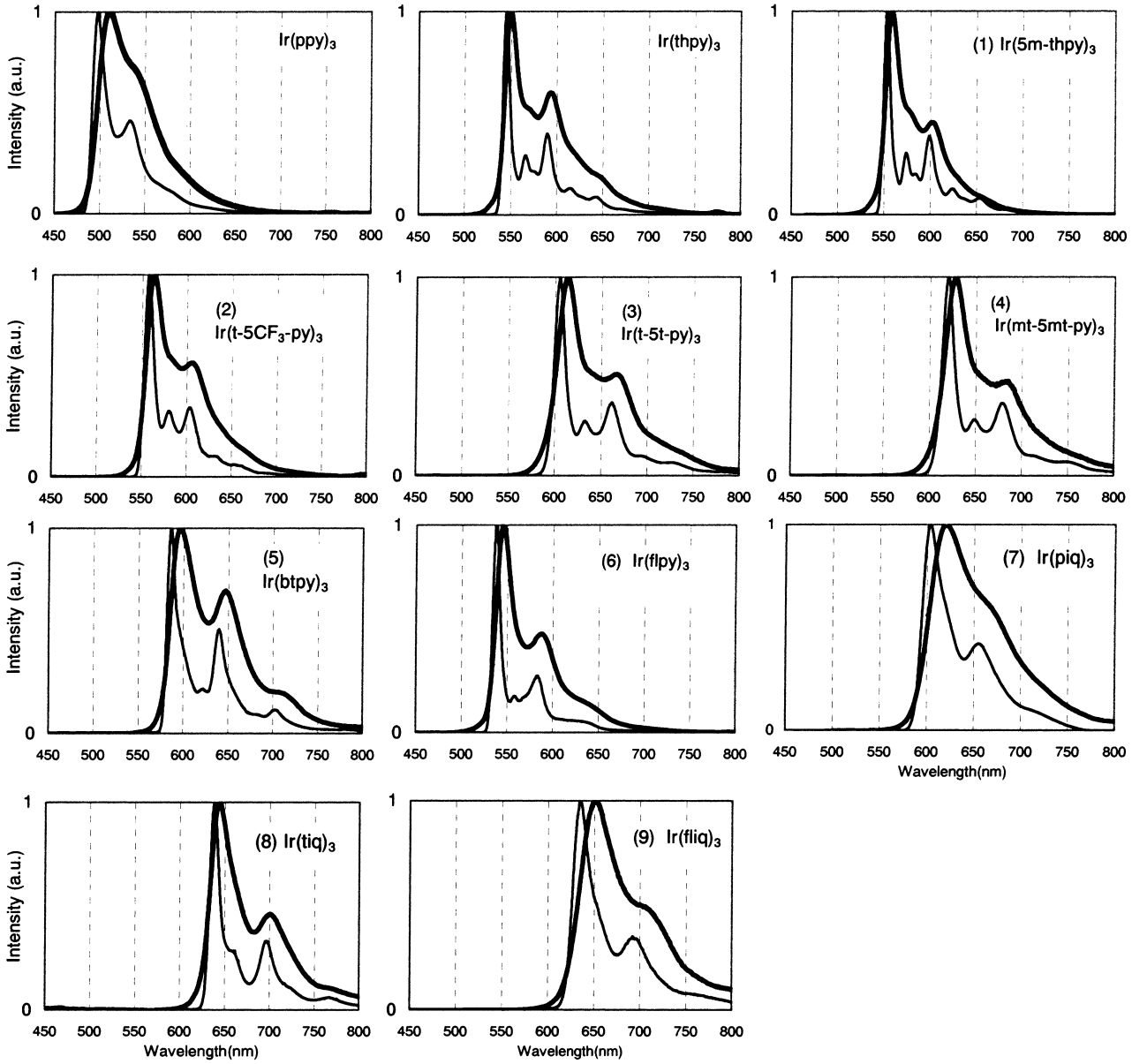

Figure 4. Normalized phosphorescence spectra of the Ir complexes at 77 K (thin lines) in toluene/ethanol/methanol (5:4:1) solutions and at 298 K (thick lines) in N_2-saturated toluene solutions.

$Ir(thpy)_3$, and the Ir isoquinoline family, **7**−**9** and $Ir(ppy)_3$. The former and the latter produce phosphorescence from the dominantly $^3\pi-\pi^*$ and the dominantly ^{3}MLCT excited state, respectively.

When the Ir complex has the dominantly $^3\pi-\pi^*$ lowest excited state, the peak wavelength of phosphorescence is assumed to be essentially dominated by the excited triplet energy of the ligand: the decrease in the triplet energy of the ligand results in the red shift of the phosphorescence spectrum of the complex. This assumption leads to the consideration that when the ligand L has triplet energy smaller than that of thpy, the iridium complex, $Ir(L)_3$, probably gives phosphorescence more red-shifted than that of $Ir(thpy)_3$. It is suggested that the triplet energy of the ligand decreases with an increase in the π conjugation space. Accordingly, we designed ligands with π-conjugation systems much larger than that of thpy: 2,5-di(thiophen-2yl)pyridine (t-5t-py) and 2-benzo[*b*]thiophen-2-yl-pyridine (btpy). The highest energy peaks of phosphorescence for these free ligands were located at 513 and 566 nm for btpy and t-5t-py at 77 K, respectively. These peaks are significantly longer than that (492 nm) of thpy. As listed in Table 2, the phosphorescence spectra of the complexes $Ir(t\text{-}5t\text{-}py)_3$ **(3)** and $Ir(btpy)_3$ **(5)** are markedly red-shifted in comparison with that of $Ir(thpy)_3$.

Molecules having intramolecular donor−acceptor (DA) systems exhibit bathochromic shifts of both absorption and emission spectra. Originally, 2-thiophen-2-yl-pyridine (thpy) itself has a DA character resulting from the interaction between an electron-rich group, thiophen, and an electron-deficient group, pyridine. The introduction of a methyl group, an electron donor group, into the thiophen moiety is considered to enhance the DA character of the ligand. Thus, we have synthesized 2-(5-methylthiophen-2-yl)pyridine (5m-thpy) and 2,5-di(5-methylthiophen-2-yl)pyridine (mt-5mt-py). The Ir complexes $Ir(mt\text{-}5mt\text{-}py)_3$ **(4)** and $Ir(t\text{-}5t\text{-}py)_3$ **(3)** are found to exhibit red shifts of the phosphorescence spectra: the phosphorescence peaks of the former and the latter are red-shifted by 8 and 14 nm, respectively, in comparison with those of $Ir(thpy)_3$ and $Ir(t\text{-}5t\text{-}py)_3$

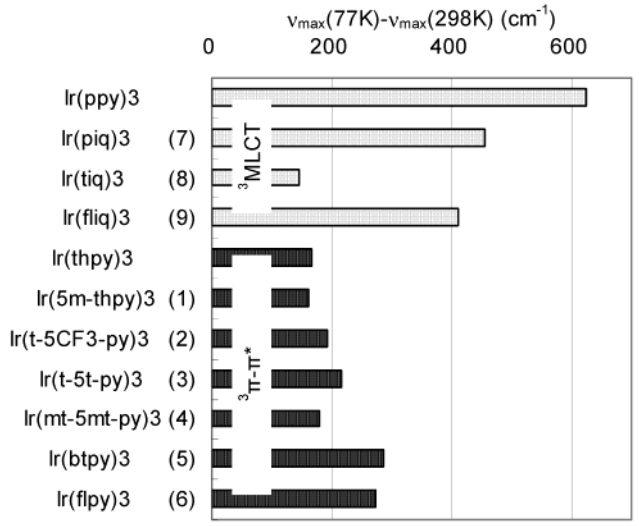

Figure 5. Rigidochromic effects of the Ir complexes. Differences in the emission peak energy between 77 K and 298 K are represented.

(**3**). These findings indicate that the introduction of the methyl group(s) into the thienyl moiety enhances the DA character of the ligand in the Ir complexes, leading to the red shift of the phosphorescence spectra.

The introduction of an electron-withdrawing group, -CF_3, into the electron-deficient pyridine moiety of thpy is also expected to increase the DA character of the ligand. In fact, both absorption and phosphorescence spectra of the iridium complex, Ir(t-5CF_3-py)$_3$ **(2)** , are located at wavelengths longer than those of Ir(thpy)$_3$ by 13 nm. From these results, it is concluded that phosphorescence spectra of the iridium complexes are red-shifted when their ligands have a large π-conjugation space and/or strong intramolecular DA interaction.

As shown in Figure 4, the phosphorescence spectra of the Ir complexes suffer the rigidochromic effect: the phosphorescence bands shift to blue on going from 298 to 77 K. The rigidochromic effect on some kinds of transition metal complexes has been previously reported.[19b,26] Because of the low viscosity of the medium at 298 K, solvent molecules in the vicinity of the excited-state molecule readily undergo reorientation by the dipole−dipole interaction within the lifetime of the excited state, resulting in the formation of the fully relaxed excited state. Thus, emission at 298 K occurs from the fully relaxed excited state. On the other hand, the excited state at 77 K emits before the solvent relaxation occurs, resulting in the rigidochromic effects on the emission spectra.

The dipole−dipole interaction between the solvent molecules and the excited state increases with an increase in the dipole moment of the excited state. Therefore, it is supposed that phosphorescence from a polar excited state can suffer a rigidochromic shift much larger than that from a less polar excited state. Figure 5 shows the difference in the energy of the highest energy vibronic band of the phosphorescence spectra at 298 and 77 K. The rigidochromic shifts of Ir(ppy)$_3$, Ir(piq)$_3$ **(7)**, and Ir(fliq)$_3$ **(9)** are found to be larger than those of other complexes, indicating that the ^{3}MLCT excited state has a more polar structure than the ligand-centered $^3\pi-\pi^*$ excited state.

3.3. Phosphorescence Yields and Lifetimes. The radiative and nonradiative rate constants, k_r and k_{nr}, are calculated from the phosphorescence yield, Φ_P, and the phosphorescence lifetime, τ:

$$\Phi_P = \Phi_{isc}\{k_r/(k_r + k_{nr})\} \quad (2)$$

$$\tau = (k_r + k_{nr})^{-1} \quad (3)$$

Here Φ_{isc} is the intersystem-crossing yield. For the iridium complexes Φ_{isc} is safely assumed to be 1.0 because of the strong spin−orbit interaction caused by heavy atom effects of iridium.[19b] In fact, no fluorescence could be detected for any complex at either 298 or 77 K. Phosphorescence peaks λ_{max}, Φ_P, and τ of the iridium complexes are listed in Table 2. The lifetimes, τ, at 77 K are 3−10 times longer than those at 298 K.

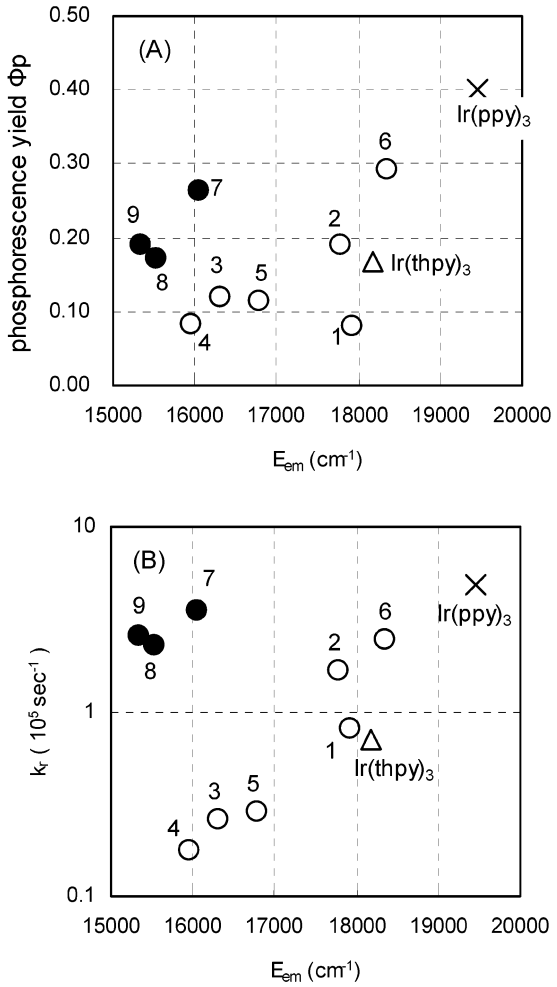

Figure 6. Plot of phosphorescence yield, Φ_P (A), and radiative rate constant, k_r (B), obtained with Ir-thiophene/fluorene family (○) and Ir-isoquinoline family (●) represented as a function of maximum emission energy of phosphorescence, E_{em} (in reciprocal centimeters) at 298 K.

Figure 6A shows the plot of the phosphorescence yield, Φ_p, vs the maximum emission energy of phosphorescence, E_{em}. It is found that (1) the yields Φ_p range from 0.08 to 0.4 and roughly tend to increase with an increase in E_{em} and (2) Φ_p of the Ir isoquinoline family is larger than that of the Ir thiophene/fluorene family in the E_{em} region 15 000−16 500 cm^{-1}.

Figure 6B shows the plot of k_r vs E_{em}. The k_r values of the Ir−thiophene/fluorene family, **1**−**6** and Ir(thpy)$_3$, increase with an increase in E_{em}, while those of the Ir isoquinoline family are almost independent of E_{em}. According to the theory of the

(26) Lees, A. J. *Comments Inorg. Chem.* **1995**, *17* (6), 319−346.

electronic transition, the k_r value is proportional to the square of the electric dipole transition moment, $\mathbf{M}_{T-S}$. First-order perturbation theory gives an approximate expression for $\mathbf{M}_{T-S}$:[27]

$$\mathbf{M}_{T-S} = \Sigma\beta_n\langle{}^1\phi_n|\mathbf{M}|{}^1\phi_0\rangle \quad (4)$$

where ${}^1\phi_n$ and ${}^1\phi_0$ are, respectively, the wave functions of the S_n and the S_0 states and $\mathbf{M}$ is the electric dipole vector. With the use of the spin−orbit coupling operator, H_{so}, and the wave function of the lowest excited triplet state, ${}^3\phi_1$, β_n is formulated as

$$\beta_n = \langle{}^1\phi_n|H_{so}|{}^3\phi_1\rangle/({}^1E_n - {}^3E_1) \quad (5)$$

where ${}^1E_n$ and ${}^3E_1$ are the energies of S_n state and the lowest excited triplet state, respectively.

Here we assume a three-state model, S_1, T_1, and S_0. Then, eq 4 is simply expressed as

$$\mathbf{M}_{T-S} = \{\langle{}^1\phi_1|H_{so}|{}^3\phi_1\rangle\langle{}^1\phi_1|\mathbf{M}|{}^1\phi_0\rangle\}/({}^1E_1 - {}^3E_1) = \alpha/({}^1E_1 - {}^3E_1) \quad (6)$$

Equation 6 predicts that, when α ($=\langle{}^1\phi_1|H_{so}|{}^3\phi_1\rangle\langle{}^1\phi_1|\mathbf{M}|{}^1\phi_0\rangle$) is approximately constant, k_r increases with a decrease in the energy difference, ${}^1E_1 - {}^3E_1$.

We find that k_r of the Ir thiophen/fluorene family increases with an increase in E_{em}. This fact is explained by assuming that the S_1 energy does not differ significantly among the complexes **1**−**5** and Ir(thpy)$_3$, and thus, the energy difference, ${}^1E_1 - {}^3E_1$, increases with the decrease in E_{em}. Actually, in the complexes **1**−**5**, spin-allowed $S_1 \leftarrow S_0$ absorption bands [log (ϵ) = ca. 4.0] are located at 460−482 nm, but phosphorescence ($S_0 \leftarrow T_1$) exhibits large bathochromic shifts ranging from 558 to 627 nm. These data provide the evidence that the energy difference ${}^1E_1 - {}^3E_1$ increases with the decrease in E_{em}, and therefore, k_r increases with an increase in E_{em}.

On the other hand, the k_r values of the Ir isoquinoline family are almost independent of E_{em}. Presumably, the energy difference ${}^1E_1 - {}^3E_1$ is approximately constant among the complexes **7**−**9** and Ir(ppy)$_3$. From the absorption data of **7**−**9** and Ir(ppy)$_3$, the energy differences between S_1 (^{1}MLCT) and T_1 (^{3}MLCT) are found to be small, ranging from 1370 to 1520 cm^{-1}. As mentioned above, we consider that the plot of k_r vs E_{em} in Figure 6B is qualitatively interpreted in terms of eq 6.

The red emissive complexes of the Ir isoquinoline family, **7**−**9**, give phosphorescence quantum yields higher than those of the complexes of the Ir thiophene/fluorene family, **3**−**5**. The high quantum yields of **7**−**9** are partly ascribed to the large k_r values, ca. 3×10^5 s^{-1}, independent of E_{em}.

The phosphorescence lifetimes, τ(77 K), measured for the Ir complexes at 77 K are represented in Table 2. The temperature dependence of the phosphorescence lifetime, τ, can be written as[19a]

$$\tau = \{k_r + k_{nr}\exp(-\Delta E/RT)\}^{-1} \quad (7)$$

Equation 7 implies that the nonradiative process has an activation barrier, ΔE. At 77 K, ΔE is much larger than RT ($\Delta E \gg 0.15$ kcal/mol); then the lifetime τ at 77 K, τ(77 K), is written by

$$\tau\,(77\text{ K}) = 1/k_r \quad (8)$$

As listed in Table 2, the values of τ(77 K) are in moderate agreement with those of $1/k_r$ obtained at 298 K.

The phosphorescence yield reflects the nature of the lowest excited state—the dominantly ^{3}MLCT excited state of the complexes **7**−**9** emits red phosphorescence with yields 0.17−0.26. These values are significantly higher than those of **3**−**4** with predominantly $^3\pi-\pi^*$ emissive excited states. Thus, we consider that the dominantly ^{3}MLCT emissive excited state is essentially important for the triply cyclometalated homoleptic iridium complexes to show pure-red and highly efficient phosphorescence.

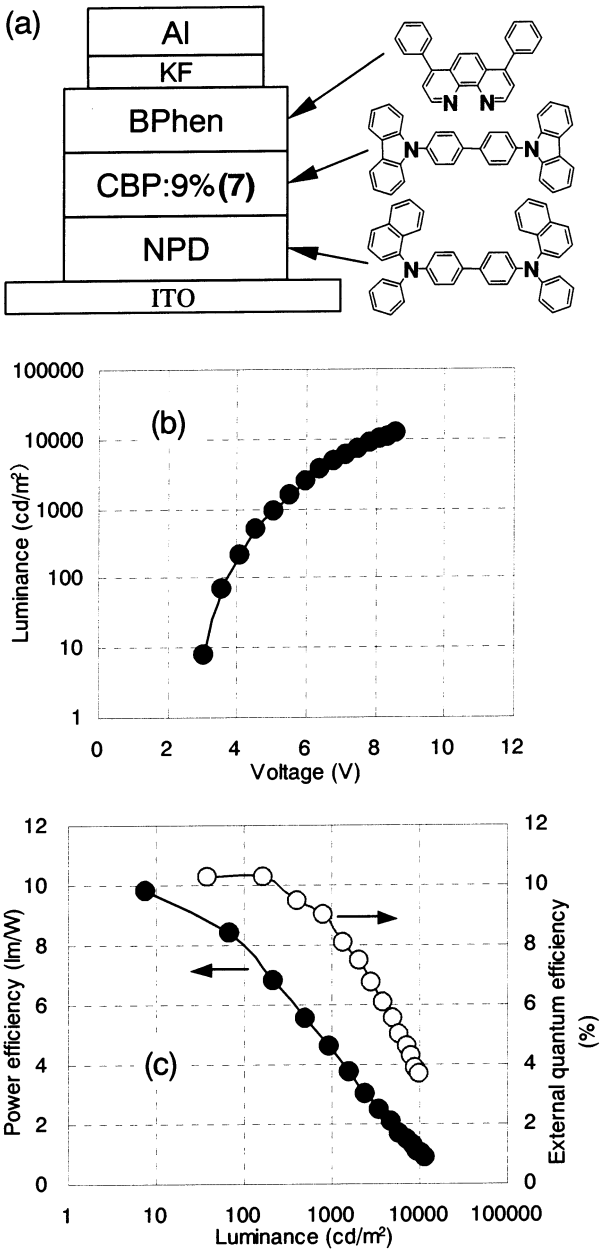

Figure 7. (a) OLED construction and molecular formulas of the compounds in each layer, (b) plot of luminance vs voltage, and (c) plots of power efficiency and external quantum efficiency vs luminance of the Ir(piq)$_3$ **(7)** device.

(27) Birks, J. B. *Photophysics of Aromatic Molecules*; Wiley-Interscience: London, 1970.

4. Performance of OLEDs with Ir(piq)$_3$ as an Emissive Dopant. In our experience, Ir-complex-doped OLEDs typically exhibit an almost linear relationship between the external quantum efficiency and the phosphorescence yield of the emissive dopant. Accordingly, Ir(piq)$_3$ **(7)** is a promising candidate as a highly efficient pure red dopant in OLEDs.

The decomposition temperature, 384 °C, of Ir(piq)$_3$ **(7)** is sufficiently high for a fabrication process by the vacuum deposition method. In addition, the small molecular weight of Ir(piq)$_3$ **(7)** in comparison with other red-emissive complexes leads to a lower sublimation temperature. In fact, Ir(piq)$_3$ **(7)** can be sublimed in a vacuum chamber without thermal decomposition.

Another significant feature of Ir(piq)$_3$ **(7)** is the short lifetime of the triplet excited state ($\tau_0 = k_r^{-1}$; 2.8 μs). In general, when phosphorescent OLED devices are operated at high current density, triplet−triplet (T−T) annihilation in the emissive layer particularly reduces the internal quantum yield.[18,28] The T−T annihilation effectively occurs when the lifetime of the triplet excited state becomes long. Therefore, Ir(piq)$_3$ **(7)**, having both a short excited-state lifetime and a high phosphorescence yield, should be advantageous to realization of highly efficient pure-red OLEDs.

An OLED device fabricated with Ir(piq)$_3$ **(7)** as a dopant in a multilayered structure is shown in Figure 7a. The layers in the device are composed of a hole transporting layer (HTL), an emissive layer (EML), an electron transporting layer (ETL), and an electron injection layer (EIL). Materials used for the device are NPD (4,4′-bis-[*N*-(1-naphthyl)-*N*-phenylamino]biphenyl for HTL (40 nm), Ir(piq)$_3$ (**7**) (9 wt%) in CBP (4,4′-*N*,*N*′-dicarbazolebiphenyl) for EML (20 nm), Bphen (4,7-biphenyl-[1,10]phenanthroline) for ETL (50 nm), and KF for EIL (1 nm).

The surface of a precoated indium−tin oxide (ITO) substrate was carefully cleaned because surface conditions strongly affect the performance of devices. The ITO substrate was ultrasonicated in a detergent solution and then in purified water. After drying in a chamber at 120 °C, the ITO surface was treated with O_2 plasma. Exposing the ITO surface to O_2 plasma increased the work function of the surface to 5.0 eV, allowing effective hole injection from the ITO anode to the organic layer. The above-mentioned materials were vacuum-deposited in turn on the ITO film at chamber pressures of less than 10^{-4} Pa, and aluminum was deposited over the KF layer as a cathode. The emissive layer (EML) was formed by co-deposition of the phosphorescent dopant, Ir(piq)$_3$ **(7)**, and the host molecule, CBP. The deposition rates were controlled with two independent quartz crystal oscillators. After fabrication, the device was confined in a small bottle containing calcium oxide desiccant to protect the device from humidity. The concentration of Ir(piq)$_3$ (**7**) in the emissive layer was 9 wt%, which afforded the optimum external efficiency, η_{ex}. At concentrations more than 9 wt%, η_{ex} tends to decrease due to self-quenching.

Panels b and c in Figure 7 display the plot of luminance vs voltage and the plots of power efficiency and external quantum yield vs luminance, respectively. The maximum luminance obtained is 11 000 cd/m^2 at 8.3 V. Power efficiency and external quantum efficiency are very high: 8.0 lm/W and 10.3% at 100 cd/m^2 and 6.3 lm/W and 9.6% at 300 cd/m^2. The CIE chromaticity coordinates are estimated to be $x = 0.68$, $y = 0.32$, which is very close to the National Television Standards Committee (NTSC) red specification. To the best of our knowledge,[18,24] the Ir(piq)$_3$ **(7)** device shows the highest published electroluminescence efficiency with pure red emission.

Summary

We have designed cyclometalated iridium complexes suitable for use as red-emissive materials in OLEDs. The phosphorescence of Ir(thpy)$_3$, which originates from the dominantly $^3\pi-\pi^*$ excited state, shifts to red by introduction of substituents and/or large congugating aromaric rings into the ligand. The k_r value of phosphorescence from the Ir(thpy)$_3$ family markedly decreases with a decrease in the energy of the lowest excited triplet state, leading to the low quantum yield of red phosphorescence. On the other hand, the Ir isoquinoline family, Ir(piq)$_3$ **(7)**, Ir(tiq)$_3$ **(8)**, and Ir(fliq)$_3$ **(9)**, is found to radiate red phosphorescence from dominantly ^{3}MLCT excited states with high quantum yields. Members of the Ir isoquinoline family produce pure-red emission spectra with λ_{max} longer than 620 nm. The OLED device doped with Ir(piq)$_3$ **(7)** exhibits very high electroluminescence efficiency as well as distinctly saturated red emission that satisfies NTSC specifications.

Supporting Information Available: Summary of the refinement details and the resulting agreement factor of Ir(piq)$_3$ and detailed procedures of the preparation, ^{1}H NMR spectra, and chemical analysis data of ligands **1**−**9** (PDF/CIF). This information is available free of charge via the Internet at http://pubs.acs.org.

JA034732D

(28) Adachi, C.; Kwong, R.; Forrest, S. R. *Org. Elect.* **2001**, *2*, 37−43.